

D-A249 612



## CUMENTATION PAGE

Form Approved  
OMB No. 0704-0188

nation is estimated to average 1 hour per response, including the time for reviewing instructions, searching existing data sources, completing and reviewing the collection of information. Send comments regarding this burden estimate or any other aspect of this burden to Washington Headquarters Services, Directorate for Information Operations and Reports, 1215 Jefferson 102, and to the Office of Management and Budget, Paperwork Reduction Project (0704-0188), Washington, DC 20503.

2. REPORT DATE  
March 20, 19923. REPORT TYPE AND DATES COVERED  
Final Technical Report

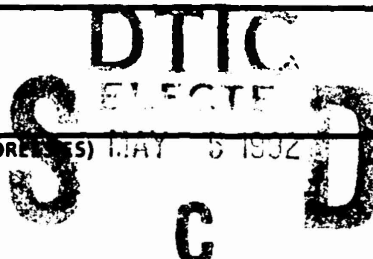
## 4. TITLE AND SUBTITLE

Development of High Efficiency Nonlinear Optical Materials

## 5. FUNDING NUMBERS

Contract Number  
DAAL03-86-K-0129

## 6. AUTHOR(S)

Robert S. Feigelson  
Roger K. Route

## 7. PERFORMING ORGANIZATION NAME(S) AND ADDRESS(ES)

Center for Materials Research  
Stanford University  
Stanford, CA 94305-4045

## 8. PERFORMING ORGANIZATION REPORT NUMBER

CMR-92-2

## 9. SPONSORING/MONITORING AGENCY NAME(S) AND ADDRESS(ES)

U. S. Army Research Office  
P. O. Box 12211  
Research Triangle Park, NC 27709-2211

## 10. SPONSORING/MONITORING AGENCY REPORT NUMBER

ARO 23577.6 MS

## 11. SUPPLEMENTARY NOTES

The view, opinions and/or findings contained in this report are those of the author(s) and should not be construed as an official Department of the Army position, policy, or decision, unless so designated by other documentation.

## 12a. DISTRIBUTION/AVAILABILITY STATEMENT

## 12b. DISTRIBUTION CODE

Approved for public release; distribution unlimited.

## 13. ABSTRACT (Maximum 200 words)

This report summarizes a five year program on the development of high efficiency nonlinear optical materials. A major objective of the program was the development of an effective crystal growth technology for barium borate (BBO) and lithium borate (LBO). A secondary objective was to grow high quality crystals to facilitate optical property determinations and nonlinear optical device development. A top-seeded solution growth technique for these two materials is described, along with an assessment of their respective growth rate limiting mechanisms. A thorough analysis of the optical scattering defects found in BBO is also included.

A supplemental task involved further development of the heat-treatment technology used to eliminate optical scattering centers from as-grown crystals of silver gallium selenide. A microchemical analysis and a mass balance model that, together, explain the dynamics of the heat-treatment process, and suggest a potential improvement in the process, are also included.

## 14. SUBJECT TERMS

Nonlinear optical materials, barium borate, lithium borate, silver gallium selenide, BBO, LBO, AgGaSe<sub>2</sub>

## 15. NUMBER OF PAGES

## 16. PRICE CODE

## 17. SECURITY CLASSIFICATION OF REPORT

UNCLASSIFIED

## 18. SECURITY CLASSIFICATION OF THIS PAGE

UNCLASSIFIED

## 19. SECURITY CLASSIFICATION OF ABSTRACT

UNCLASSIFIED

## 20. LIMITATION OF ABSTRACT

UL

NSN 7540-01-280-5500

Standard Form 298 (Rev. 2-89)  
Prescribed by ANSI Std Z39-18

92 4 27 270

The Board of Trustees of the  
Leland Stanford Junior University  
Center for Materials Research  
Stanford, California 94305-4045  
Santa Clara, 12th Congressional District

Final Technical Report  
on  
**DEVELOPMENT OF HIGH EFFICIENCY  
NONLINEAR OPTICAL MATERIALS**  
ARO: DAAL03-86-K-0129  
CMR-92-2

for the period  
September 1, 1986 through December 31, 1991

Submitted to  
U.S. Army Research Office  
Materials Division  
Research Triangle Park, NC 27709

Principal Investigator:

  
Robert S. Feigelson, Professor (Res.)  
Center for Materials Research  
Stanford, California 94305-4045  
(415) 723-4007

March 1992

APPROVED FOR PUBLIC RELEASE;  
DISTRIBUTION UNLIMITED

A-1

## **ABSTRACT**

This report summarizes a five year program on the development of high efficiency nonlinear optical materials. A major objective of the program was the development of an effective crystal growth technology for barium borate (BBO) and lithium borate (LBO). A secondary objective was to grow high quality crystals to facilitate optical property determinations and nonlinear optical device development. A top-seeded solution growth technique for these two materials is described, along with an assessment of their respective growth rate limiting mechanisms. A thorough analysis of the optical scattering defects found in BBO is also included.

A supplemental task involved further development of the heat-treatment technology used to eliminate optical scattering centers from as-grown crystals of silver gallium selenide. A microchemical analysis and a mass balance model that, together, explain the dynamics of the heat-treatment process, and suggest a potential improvement in the process, are also included.

**THE VIEW, OPINIONS, AND/OR FINDINGS CONTAINED IN THIS REPORT ARE THOSE OF THE AUTHORS AND SHOULD NOT BE CONSTRUED AS AN OFFICIAL DEPARTMENT OF THE ARMY POSITION, POLICY, OR DECISION, UNLESS SO DESIGNATED BY OTHER DOCUMENTATION.**

## FORWARD

This is the final technical report on DAAL03-86-K-0129, "Development of High Efficiency Nonlinear Optical Materials," which began at Stanford University on September 1, 1986. The overall objective of the program was the development of new high efficiency nonlinear optical materials. Initial emphasis was placed on the growth of the low temperature phase of barium borate,  $\beta\text{-BaB}_2\text{O}_4$ , which is a highly nonlinear material important for harmonic generation and mixing applications in the visible and UV. With the discovery of lithium tri-borate ( $\text{LiB}_3\text{O}_5$ ), a relatively newer nonlinear material with a somewhat different set of applications, also in the visible and UV, we included an increasing emphasis on this material as well. Research studies on these two materials were carried out under this program over a period of 44 months, concluding on April 30, 1990.

On May 1, 1990, an additional \$20K supplemental allocation and a program extension were received to facilitate Ph. D. dissertation research relating to diffusion phenomena in the infrared nonlinear optical material silver gallium selenide ( $\text{AgGaSe}_2$ ), work which derived from other ARO programs, DAAG29-84-K-0071 and DAAL03-88-K 0113. This supplemental project continued through December 31, 1991.

The program has been highly successful both in the visible/UV materials, barium borate and lithium borate, and in the infrared material silver gallium selenide. When it began, there was little direct experience or activity in this country on the crystal growth and characterization of either barium borate or lithium borate. Research on the preparation of these materials under this program resulted in the first US-grown samples for optical studies. During this time, a viable crystal growth technology was developed for each, and successfully transferred to industry. The supplemental work on silver gallium selenide has resulted in a significant improvement in our understanding of the thermodynamics of this material and in the heat-treatment processing that is necessary for its use.

## TABLE OF CONTENTS

Form 298	i
Abstract	ii
Forward	iii
Table of Contents	iv
I. Introduction	1
II. Research Results	2
A. Barium Borate	2
1. Objectives	2
2. Background	2
3. Phase Equilibria and Solvent Studies	2
4. Crystal Growth Experiments	4
5. Summary of Results	7
6. References: Part A	7
B. Lithium Borate	9
1. Objectives	9
2. Background	9
3. Phase Equilibria	11
4. Crystal Growth Experiments	11
5. Results	16
6. Discussion	19
7. Summary of Results	22
8. References: Part B	23
C. Silver Gallium Selenide	25
1. Objectives	25
2. Background	25
3. Chemical Analysis of the Heat-Treatment Process	27
4. A Chemical Mass Balance Model for the Heat-Treatment Process	30
5. Summary of Results	33
6. References: Part C	33
III. Conclusions and Recommendations for Further Study	35
IV. Publications	37
V. Participating Personnel	38
VI. Report of Inventions	39

## I. INTRODUCTION

### A. OBJECTIVES

The overall objective of the program was the development of new high efficiency nonlinear optical materials. Initial emphasis was placed on the growth of the low temperature phase of barium borate, BaB<sub>2</sub>O<sub>4</sub> (BBO), which is a highly nonlinear material important for harmonic generation and mixing applications in the visible and UV. When the program began, there was little direct experience with this material beyond several joint studies that had been made on a few crystals from Fujian in the PRC. The initial, and ultimately the major, program goal became the development of a reproducible crystal growth technique that would yield useable size crystals and be transferable to the commercial sector. Secondary objectives related to improving the optical quality : early crystals all contained inclusions in varying densities that we later determined were caused by solvent entrapment on the growing interface. The approach taken was the development of high thermal gradient solution growth furnaces that would result in the most stable growth interfaces and permit the highest possible growth rates, and the identification of an optimum solvent.

With the discovery of lithium tri-borate (LiB<sub>3</sub>O<sub>5</sub>), a relatively newer nonlinear material with a somewhat different set of applications, also in the visible and UV, we included the objective of growing test crystals of this material and developing a similar growth technology, as well. Even less was known about the growth properties of LBO when we began beyond the phase equilibrium in the Li<sub>2</sub>O-B<sub>2</sub>O<sub>3</sub> system which had been worked out twenty years earlier. Our approach was to use similar high gradient solution growth furnaces to evaluate several possible solvent systems and to determine the range of parameters over which the desired phase could be grown.

The supplemental program on silver gallium selenide extended work already in progress (under DAAL03-88-K-0113) on improving the heat-treatment processing of this material through an increased understanding of the chemistry and kinetic behavior of the heat-treatment process.

## II. RESEARCH RESULTS

### A. BARIUM BORATE

#### 1. Objectives

Program objectives relating to barium borate were two-fold: 1) learning how to grow large, high optical quality crystals by the top-seeded solution growth (TSSG) method at reasonable growth rates; and 2) developing an alternative growth method which would overcome some of the difficulties intrinsic to the TSSG method.

#### 2. Background

Barium borate, a relatively new and important material for nonlinear optical applications in the visible and ultraviolet regions<sup>[1-7]</sup>, has a number of physical properties which make it particularly attractive, including large effective SHG coefficients ( $d_{eff} = 6 \times d_{eff}$  for KDP at 1.06 mm), a wide transparent waveband (190 nm to 3500 nm), low dispersion, a large birefringence, high damage thresholds ( $13.5 \pm 2$  GW/cm<sup>2</sup> for 1 ns pulses at 1.06 mm and  $7.0 \pm 1$  GW/cm<sup>2</sup> for 250 ps pulses at 0.532 mm), and high optical homogeneity ( $D \approx 10^{-6}$ /cm). It has good mechanical properties, polishes well and, although it appears to be weakly water soluble, does not appear to be hygroscopic under reasonably dry laboratory conditions.

#### 3. Phase Equilibria and Solvent Studies

Barium borate is known to exist in two phases, a high temperature  $\alpha$ -phase and the low temperature  $\beta$ -phase [8] that is useful for nonlinear applications. The crystal structure of the low temperature  $\beta$ -phase of barium borate consist of  $(B_3O_6)^{3-}$  units which form nearly planar rings which are the key to its optical properties. Barium borate exists as an intermediate compound in the BaO-B<sub>2</sub>O<sub>3</sub> pseudobinary system and melts congruently at 1096° C, [9] but due to the structural reordering that occurs during the phase transition at 925° C, it must be grown from solution below 925° C. In our initial experiments, we determined that growth from solutions containing an excess of either BaO and B<sub>2</sub>O<sub>3</sub> resulted in very poor crystal quality.

Our success in growing BaB<sub>2</sub>O<sub>4</sub> came with the discovery that Na<sub>2</sub>O is a suitable solvent for this material. The Na<sub>2</sub>O system [10] offers a much wider cooling range than the BaO-B<sub>2</sub>O<sub>3</sub> system and it was quickly found to yield crystals of substantially higher quality, Fig. 1. Solution viscosities in the Na<sub>2</sub>O system were found to be larger than one would like and this led us to carry out a limited set of experiments with BaF<sub>2</sub> added to the

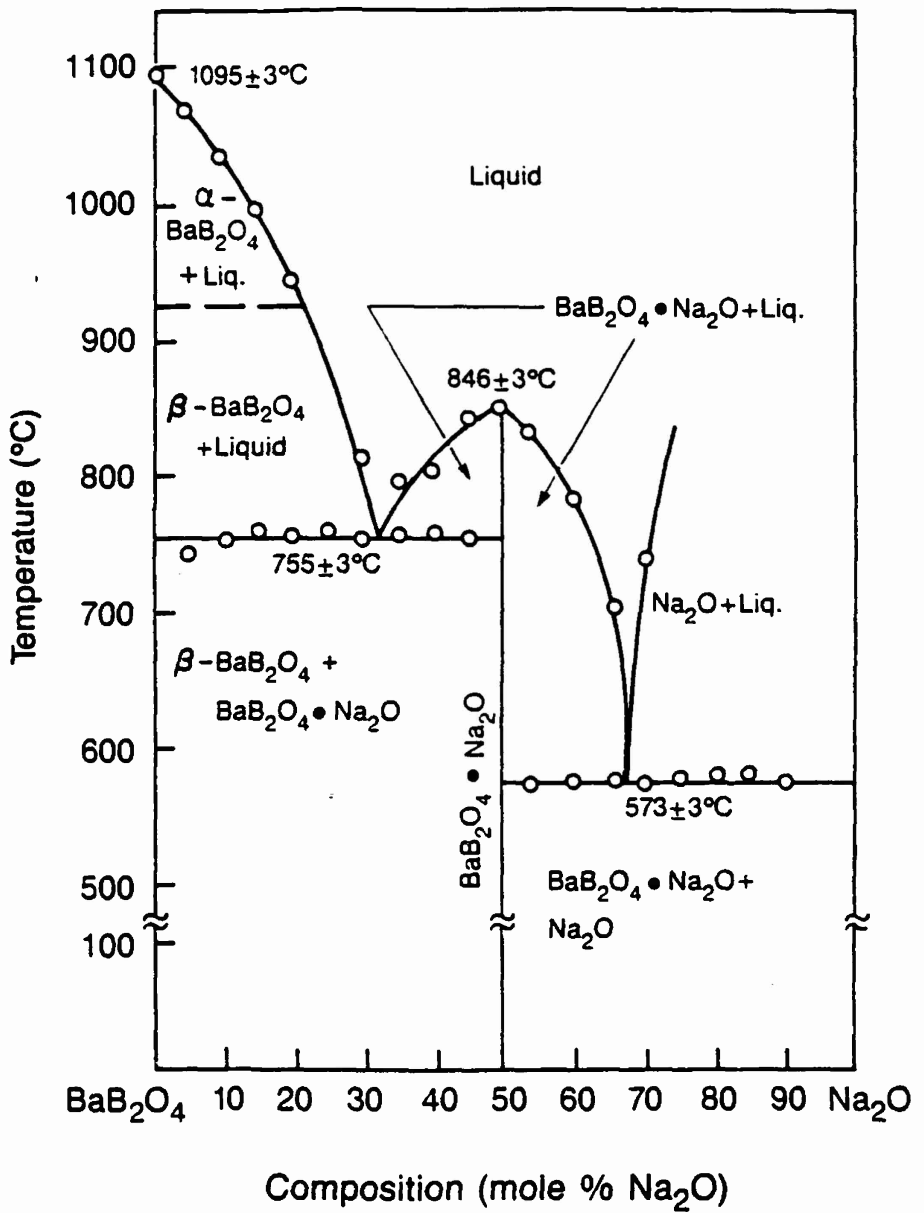


Fig. 1. Phase equilibria in the  $\text{BaB}_2\text{O}_4$ - $\text{Na}_2\text{O}$  system after Huang and Liang. [10]

$\text{BaB}_2\text{O}_4$ - $\text{Na}_2\text{O}$  system as a viscosity modifier. However, no substantial improvements in crystal quality were found, and for the bulk of the program, we concentrated on the use of pure  $\text{BaB}_2\text{O}_4$ - $\text{Na}_2\text{O}$  melts with approximate starting compositions of 18-20 at %  $\text{Na}_2\text{O}$  and liquidus temperatures in the 925° C range.

#### 4. Crystal Growth Experiments

The top-seeded solution growth (TSSG) method [11] was used for the bulk of our studies. Best results were obtained from SiC-heated box furnaces having steep radial and axial temperature gradients. Because the solubility of  $\text{BaB}_2\text{O}_4$  increases with temperature in the  $\text{Na}_2\text{O}$  solvent system, growth of  $\beta$ - $\text{BaB}_2\text{O}_4$  from solution was controlled using a standard slow cooling technique. Crystal growth experiments were carried out using c-axis and the y-axis seeds.

Initially, c-axis crystals were grown without pulling and these assumed the shallow lens shape typical of the  $\text{BaB}_2\text{O}_4$  crystals grown in the PRC. Thicker crystals were grown by pulling slowly during growth. Typically, we used a cooling rate of 2° C/day and a pulling rate of 0.5-1.0 mm/day with reasonably good results. Growth was continued until sufficient length or weight was achieved to yield useful size crystals. On average, we were able to cool the melts 70-85° C and pull approximately 15 mm before the onset of growth interface instability, which turned out to be a major limitation to c-axis growth.

With these growth parameters, c-axis  $\beta$ - $\text{BaB}_2\text{O}_4$  crystals, free of secondary grains, were readily grown in sizes exceeding 75 mm diameter and weighing as much as 185 g from melts in the 1200 g range, Fig. 2. The tops of the crystals always contained shallow, well-developed facets reflecting the three-fold symmetry along the c-axis. Growth interfaces varied from concave to convex, depending on growth conditions. Most were smooth and contained three rounded facets. Although the seed crystals cleaved along the (001) during cooling, c-axis crystals rarely fractured.

We also demonstrated that y-axis crystals could be grown from  $\text{Na}_2\text{O}$  solutions. Due to growth rate anisotropy, boule cross-sections were more elliptical and faceting on the top surface of the boule was less pronounced. A major advantage of y-axis boules was that they grew in a nearly cylindrical shape when pulled. Using relatively smaller 470 g melts, we were able to pull y-axis crystals as large as 53 g and 15 mm long. Unfortunately, y-axis crystals tended to fracture along the basal planes during cooling.

Most  $\beta$ - $\text{BaB}_2\text{O}_4$  contained internal microscopic defects, c-axis crystals having a higher density in a core region. Y-axis crystals display a less pronounced core. These defects were studied extensively by optical microscopy and electron microscopy. Energy dispersive SEM analysis showed the microscopic defects to be inclusions with the major

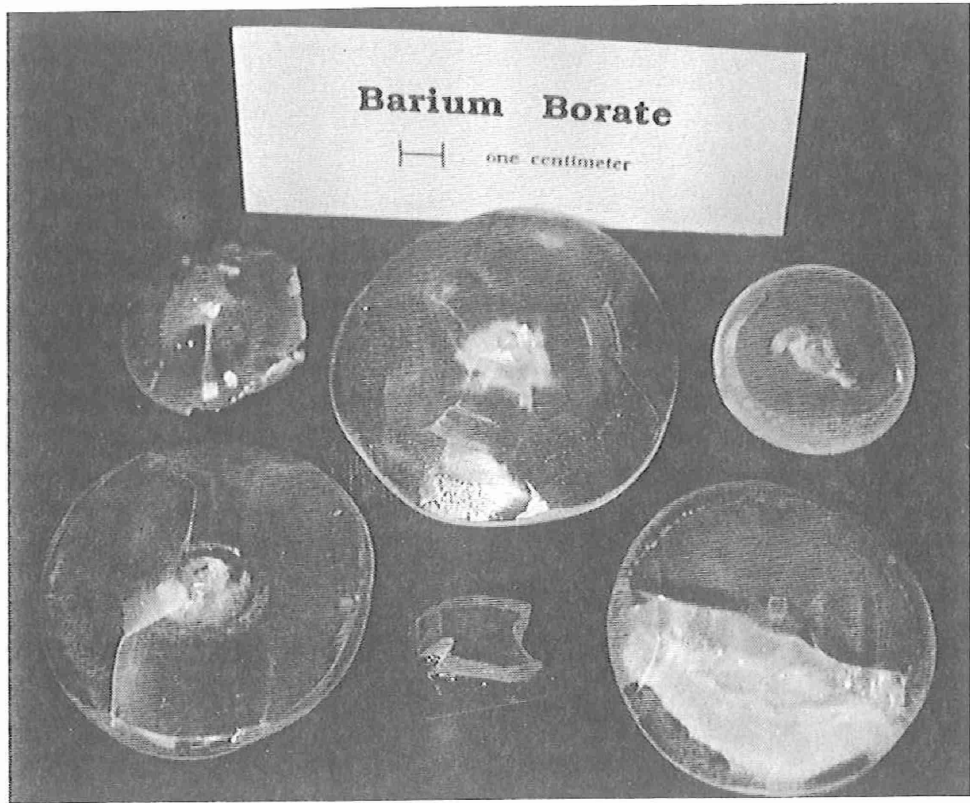


Fig. 2. BBO crystals as large as 185 g grown from Na<sub>2</sub>O solution by the TSSG method.

constituent consisting of sodium. These studies were the first to conclusively demonstrate that the defects in  $\beta$ -BaB<sub>2</sub>O<sub>4</sub> are caused by small amounts of entrapped solvent.

Because the top-seeded solution growth method is not an isothermal technique, it was found difficult to analyze using isothermal phase equilibria and simplified modeling. Instead, we resorted to phenomenological modeling to develop an optimum set of growth parameters. In one set of experiments on the effects of seed rotation, better mixing and a greater sweeping of melt across the growth interface were shown to reduce inclusions. While constant seed rotation rates were not particularly effective in accomplishing this, computer-controlled periodic reversals in seed rotation were found to be effective in decoupling forced convection (sweeping rate) from irregular thermal convection and gave us a means to independently control melt sweeping on the growth interface. The entire set of experiments was quite encouraging - boule morphology was improved considerably, growth interfaces were exceptionally smooth, and He-Ne laser scattering indicated that major fractions of these crystals grew virtually free of inclusions.

The exact mechanism leading to the formation of solvent inclusions and voids in bulk BBO crystals could not be determined with certainty. Interface instability due to thermal fluctuations and reduced thermal gradients as growth proceeded were considered to be the most likely. However, other possibilities such as insoluble particles in the melt, poisoning of the growth interface by impurities and evolution of dissolved gas at the growth interface could not be eliminated.

A parallel study on the growth of BBO by the laser-heated pedestal growth (LHPG) method, which was ongoing at the time this program began, sought to determine if high quality single crystal fibers of BBO could be grown by the LHPG method. At the time, it was believed that BBO had to be crystallized from solution at temperatures below its  $\alpha$ - $\beta$  phase transition temperature of 925° C. High optical quality BBO fibers were, in fact, grown by us at temperatures around 925° C using B<sub>2</sub>O<sub>3</sub> as the solvent phase. Using the LHPG apparatus to evaluate a number of other solvents, we found that the low temperature  $\beta$  phase could be grown from Na<sub>2</sub>O solutions with liquidus temperatures exceeding 1050° C, in clear contradiction to the established phase equilibria. [12] This work was not pursued in our laboratory because of manpower limitations and the fact that the high temperature Na<sub>2</sub>O-grown fibers still contained optical scattering defects. However, it did stimulate other researchers to duplicate our results and explore the method somewhat further. In 1989, Onishi found that  $\beta$ -BBO fibers could be grown from pure melts using starting material prepared by chloride decomposition. [13] This very important finding, which eventually led to the discovery that even larger crystals could be grown metastably from the melt, [14,15] was made possible by our initial work using the LHPG method.

## 5. Summary of Results

1. Large single crystals of  $\beta$ -BaB<sub>2</sub>O<sub>4</sub> were grown from 80 at % BaB<sub>2</sub>O<sub>4</sub> - 20 at % Na<sub>2</sub>O solutions using both c-axis and y-axis seeds.
2. High thermal gradient, SiC-heated furnaces were shown to allow higher growth rates than low gradient furnaces. Optical defect densities were lower in high gradient furnaces, and crystals could be grown in larger dimensions before the onset of interface instability.
3. Optical defects were thought to be due to solvent entrappment on the growth interface, perhaps caused by local instabilities due to irregular thermal convection. Only trace amounts of other contaminants were found at the defect sites.
4. Mass transport is thought to be the rate limiting mechanism in this system since solution viscosities are known to be relatively high. However, fluoride flux modifiers did not result in improved crystal quality or reduction in the density of solvent inclusions.
5. Microsegregation (banding) due to irregular convection was not detected. Rather, vertical cell boundaries suggesting constitutional supercooling were seen. Both mass transport and constitutional supercooling problems would be reduced if a solvent having lower viscosity could be found.
6. Computer-controlled periodic reversals on seed rotation were demonstrated to enhance sweeping of the melts across the growth interfaces and greatly reduce the density of solvent inclusions.

*The research study on the growth of barium borate is described in detail in publication numbers 1-4.*

## 6. References: Part A

1. C.-T. Chen, B. Wu, G. You, and Y. Huang, "High-efficiency and wide-band second-harmonic generation properties of new crystal  $\beta$ -BaB<sub>2</sub>O<sub>4</sub>," Dig. Tech. Papers XIII IQEC, Paper MCC5 (1984).
2. C. Chen, B. Wu, A. Jiang, and G. You, "A new type ultraviolet SHG crystal  $\beta$ -BaB<sub>2</sub>O<sub>4</sub>," Sci Sinica (Ser B) **28**, 235 (1985).
3. J.-K. Zhu, B. Zhang, and S.-H. Liu, "A study of second harmonic generation coefficients and ultraviolet absorption edge of barium borate crystal," SPIE Conf. on basic properties of Optical Materials, Gaithersburg, Md, May 7-9, 1985.
4. K. Kato, "Second-harmonic generation to 2048 Å in  $\beta$ -BaB<sub>2</sub>O<sub>4</sub>," IEEE J. Quantum. Electron. **22**, 1013 (1986).

5. K. Miyazaki, H. Sakie, and T. Sato, "Efficient deep-ultraviolet generation by frequency doubling in  $\beta$ -BaB<sub>2</sub>O<sub>4</sub> crystals," Opt. Lett. **11**, 797 (1986).
6. G. Zhang, C. Jin, F. Lin, C. Chen and B. Wu, "Second harmonic generation of a copper vapor laser by using a beta-barium borate (BaB<sub>2</sub>O<sub>4</sub>) crystal," Guangxue Xuebao **4**, 513 (1984).
7. C. Chen, Y. X. Fan, R. C. Eckardt, and R. L. Byer, "Recent developments in  $\beta$ -BaB<sub>2</sub>O<sub>4</sub>," Proc. of SPIE Conf. on Lasers, San Diego, Calif., July 1986, SPIE **684**(4) (to be published).
9. E. M. Levin and H. F. McMurdie, "The system BaO-B<sub>2</sub>O<sub>3</sub>," J. Res. Natl. Bur. Stand. **42**, 131 (1949).
8. J. Liebertz and S. Stahr, "Zur tieftemperaturphase von BaB<sub>2</sub>O<sub>4</sub>," Z. Kinstall. **165**, 91 (1983).
10. Q.-Z. Huang and J.-K. Liang, "The crystal growth of barium borate low temperature phase and the study of phase diagrams of related systems," Acta Physica Sinica **30**(4), 559 (1981).
11. D. Elwell and H. J. Scheel, Crystal Growth from High Temperature Solutions, ed. Academic Press Inc., London, New York, San Francisco (1975).
12. N. Onishi, Ceramics (Japan) **24**, 319 (1989).
13. K. Itoh, F. Marumo and Y. Kuwano, " $\beta$ -barium borate single crystals grown by a direct Czochralski method," J. Crystal Growth **106**, 728 (1990).
14. Y. Kozuki and M. Itoh, "Metsastable crystal growth of the low temperature phase of barium metaborate from the melt," J. Crystal Growth **114**, 683 (1991).

## B. LITHIUM BORATE

### 1. Objectives

Program objectives relating to lithium borate were twofold: 1.) learning how to grow crystals of the correct  $\text{LiB}_3\text{O}_5$  phase in sizes large enough for accurate physical and optical property determinations, and 2.) elucidating the thermodynamic and melt rheological factors that severely limit achievable growth rates to fractions of a millimeter per day.

### 1. Background

Lithium triborate ( $\text{LiB}_3\text{O}_5$ ), commonly known as LBO, is a relatively new nonlinear optical material that combines wide transparency extending into the UV, moderately large nonlinear optical coefficients, high laser damage threshold and good chemical/mechanical properties. The advantageous nonlinear optical properties and potential applications of this material were first reported by Chen et al in 1989 [1] as an extension of his work on BBO. High conversion efficiencies have recently been demonstrated in noncritical second harmonic conversion of  $1.064 \mu\text{m}$  radiation in high peak power, Q-switched operation, [2] and in high average power, cw operation. [3] In 1990, crystals became available in limited sizes, on the order of one centimeter maximum, on the commercial market. However, when this program began, there were no sources available in this country and researchers in nonlinear optics had to rely on a few crystals from the PRC and university-based crystal growth efforts such as ours.

LBO was first reported by Mazetti and Carli in 1926 [4], and later by Rollet and Bouaziz [5] in 1955. In 1978, Konig and Hoppe [6] determined the crystal structure of the 1-3-5 phase which is orthorhombic, belonging to space group  $\text{Pbn}2_1$ . In contrast to BBO, the structural elements that make up the LBO structure are  $(\text{B}_3\text{O}_7)^{5-}$  rings in which one of the three borons is tetrahedrally coordinated, as shown in Fig. 1. The tetrahedral bonding causes the  $(\text{B}_3\text{O}_7)^{5-}$  rings to form endless spiral chains along the c-axis, indicated by its two-fold screw symmetry in that direction, and this is responsible for the large out-of-plane z-component in the second order polarizability that makes possible non-critical phasematched interactions.

Lithium borate has good mechanical properties: it is slightly harder than BBO (6 vs. 4.5 on the Moh scale, respectively), it polishes well, and in contrast to BBO, its surfaces do not degrade with time due to reactivity with water vapor in the ambient atmosphere.

● Boron  
○ Oxygen  
◎ Oxygen or hydroxy ion

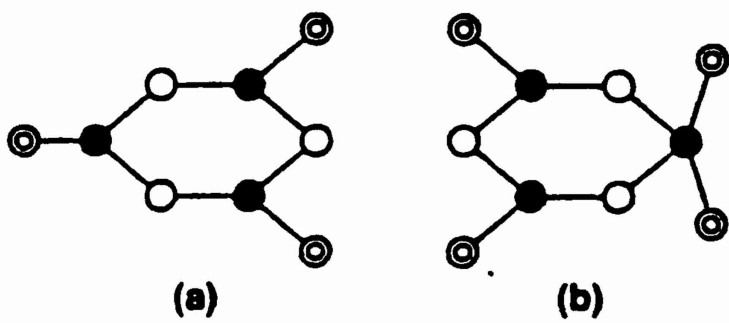


Fig. 1. Molecular configurations of a) planar  $(B_3O_6)^{3-}$  ring found in BBO, and b) the nonplanar  $(B_3O_7)^{5-}$  ring found in LBO.

### 3. Phase Equilibria

In 1958, Sastry and Hummel [7] published the first accurate determination of the phase equilibria in the  $\text{Li}_2\text{O}$ - $\text{B}_2\text{O}_3$  pseudobinary system, as shown in Fig. 2. They were the first to grow small needles of the 1-3-5 phase, which they solidified from excess  $\text{B}_2\text{O}_3$  solution, and which they used for optical property determinations. They found the 1-3-5 ( $\text{LiB}_3\text{O}_5$ ) phase to decompose peritectically at  $834 \pm 4^\circ \text{C}$ . The low temperature decomposition postulated to occur around  $595^\circ \text{C}$  has not been verified in subsequent studies by other researchers, and the 1-3-5 composition is now felt to be a stable phase down to room temperature. An important part of their work was the determination of the powder x-ray diffraction patterns for all of the phases on the  $\text{B}_2\text{O}_3$ -rich side of the  $\text{Li}_2\text{O}$ - $\text{B}_2\text{O}_3$  phase diagram.

In 1988/9, two years after this program began, Jiang et al. [8] reported the growth of larger LBO crystals from viscosity-modified  $\text{B}_2\text{O}_3$  fluxes that they did not identify. In 1989, Chen et al. reported growth from  $\text{MoO}_3$  solutions. [9] However,  $\text{MoO}_3$  was reported to produce crystals with flux inclusions by others who explored this route. [10] Also in 1989, Zhao et al. reported the growth from solutions modified by  $\text{LiF}$  and other unidentified additives. [11]

### 4. Crystal Growth Experiments

According to the phase equilibria of Sastry and Hummel op cit., LBO can be grown from excess  $\text{B}_2\text{O}_3$  solutions by using slow cooling. Initially, we undertook the growth of LBO from  $\text{B}_2\text{O}_3$ -rich melts using 125-250 g charges synthesized from  $\text{Li}_2\text{CO}_3$  and  $\text{B}_2\text{O}_3$  in high gradient TSSG furnaces like those used for the growth of BBO. Axial and radial temperature gradients were in the range of  $20^\circ \text{C/cm}$  and  $25^\circ \text{C/cm}$ , respectively. Melts compositions were chosen to place the liquidus around  $800^\circ \text{C}$ , which corresponded to compositions in the 90%  $\text{B}_2\text{O}_3$  range. X-ray powder diffraction analysis of the first crystals grown from these solutions indicated that the phase produced was not the desired 1-3-5 phase.  $\text{B}_2\text{O}_3$ -rich solutions in the  $\text{Li}_2\text{O}$ - $\text{B}_2\text{O}_3$  system were found to tolerate considerable undercooling, and without the correct 1-3-5 phase as a substrate,  $\text{Li}_4\text{B}_{10}\text{O}_{17}$ , a neighboring phase slightly richer in Li and slightly higher in its (also peritectic) decomposition temperature, was found to crystallize metastably instead. The desired 1-3-5 phase was successfully grown only after a polycrystalline 1-3-5 sample was first synthesized by recrystallizing a glass of the desired composition and using it as a polycrystalline seed.

Growth solutions with liquidus temperatures in the  $800^\circ \text{C}$  range were found to be quite viscous. Preliminary rotating cylinder melt rheological studies in our laboratory

$\text{Li}_2\text{O}-\text{B}_2\text{O}_3$

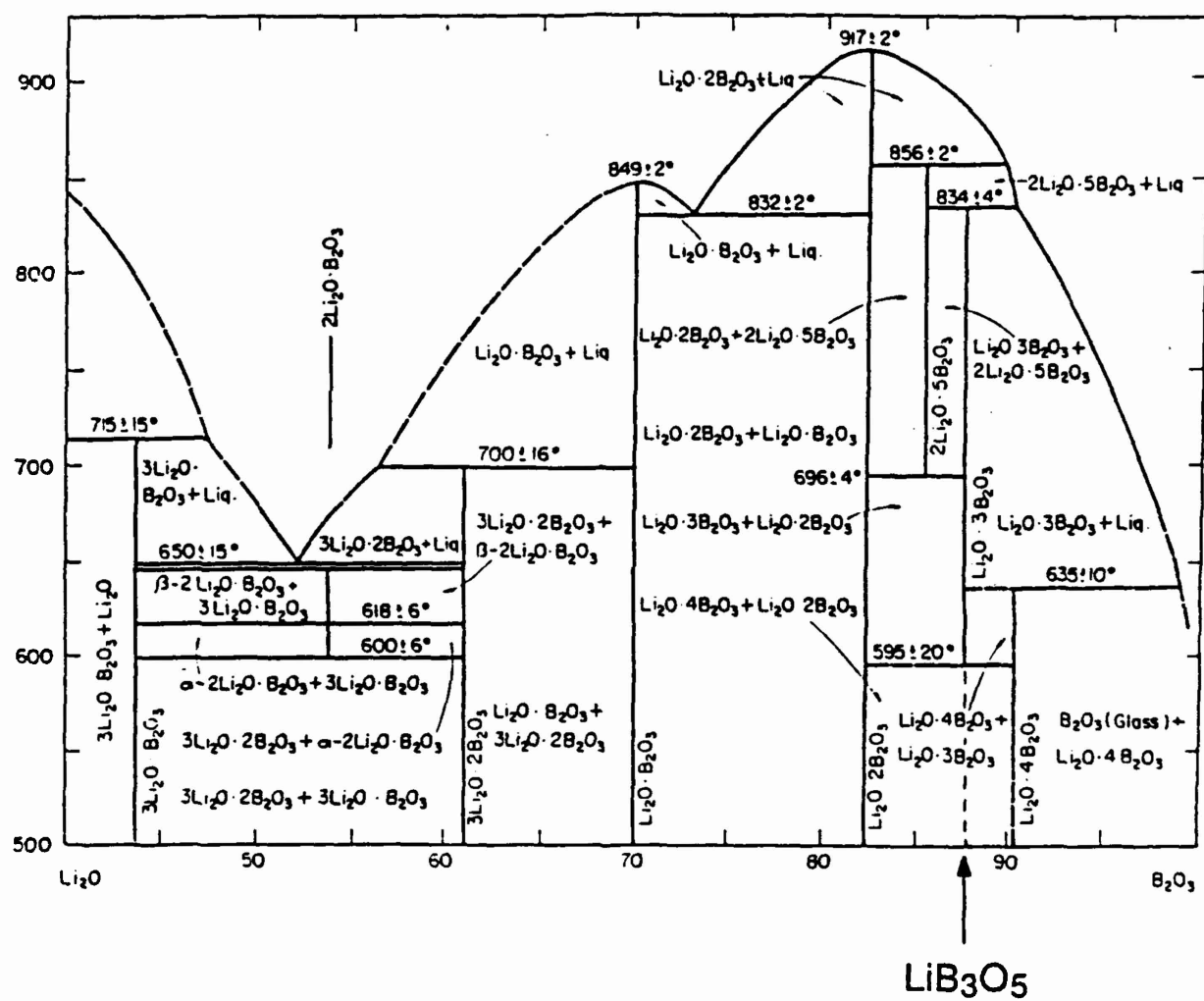


Fig. 2.  $\text{Li}_2\text{O}-\text{B}_2\text{O}_3$  phase diagram after Sastry and Hummel.<sup>[7]</sup>

found melt viscosities as high as 80 poise near the point of saturation (800° C), in general agreement with Shartsis et al. [11]. Viscosities were measured at several different shear rates, but the values obtained were within  $\pm 5\%$ , suggesting that the melts were Newtonian. The melt viscosities were found to display typical Arrhenius type behavior, with an activation energy of 43 Kcal/mole, as shown in Fig. 3. Room temperature simulation experiments using glycerine/water mixtures of equal viscosity, revealed that mixing due to seed rotation was minimal, Fig. 4. This finding suggested that a very thick diffusion boundary layer could be expected during growth, and that very low growth rates corresponding to the early literature reports [1,12] could be expected.

Anticipating that high growth solution viscosities would present a problem, a series of experiments on the growth behavior from modified solutions was included in this study. The well known viscosity-reducing flux modifier, LiF, which shares a common cation with LBO was added to test solutions in amounts to 5 wt %. In a series of solidification experiments, clear benefits over the pure oxide system were not obvious, even though the solution viscosities appeared to have been lowered by a detectable amount. LiF-modified solutions exhibited a strong tendency to develop numerous elongated prismatic needles, and the stability of the crystal growth interfaces was poor. We also studied test solutions with up to 25 at % Na<sub>2</sub>O (partially replacing Li<sub>2</sub>O) as a viscosity modifier. Somewhat better crystal morphology was achieved using these solution compositions. However, in neither case was a clear advantage over the use of pure B<sub>2</sub>O<sub>3</sub> apparent, and the bulk of the growth studies were carried out using pure B<sub>2</sub>O<sub>3</sub> as a solvent.

Initial growth experiments were carried out using randomly oriented crystallites as seeds. When large enough crystals became available, a systematic study was undertaken to study the effects of seed orientation on crystal quality and growth behavior. We sought to explore growth along the low index crystallographic directions, of which there are seven possibilities in LiB<sub>3</sub>O<sub>5</sub> which has orthorhombic symmetry.

Seed introduction and the initiation of growth in the case of LBO was found to be much more difficult than the case of BBO in which the melt can be brought to saturation very precisely. Its very sluggish dissolution and growth kinetics combined with a strong tendency to supercool make it extremely tedious to bring an LBO melt to the point of saturation prior to seed introduction. A hot dip technique in which the saturation temperature needed to be determined to only within a few degrees was used instead. In this method, the melts were superheated above the estimated saturation temperature by 10-15° C, the seed was dipped and held for approximately 10 minutes at temperature, and finally the furnace was cooled rapidly to approximately 2° C below the estimated saturation temperature. The slight amount of dissolution that occurred at elevated temperature reduced

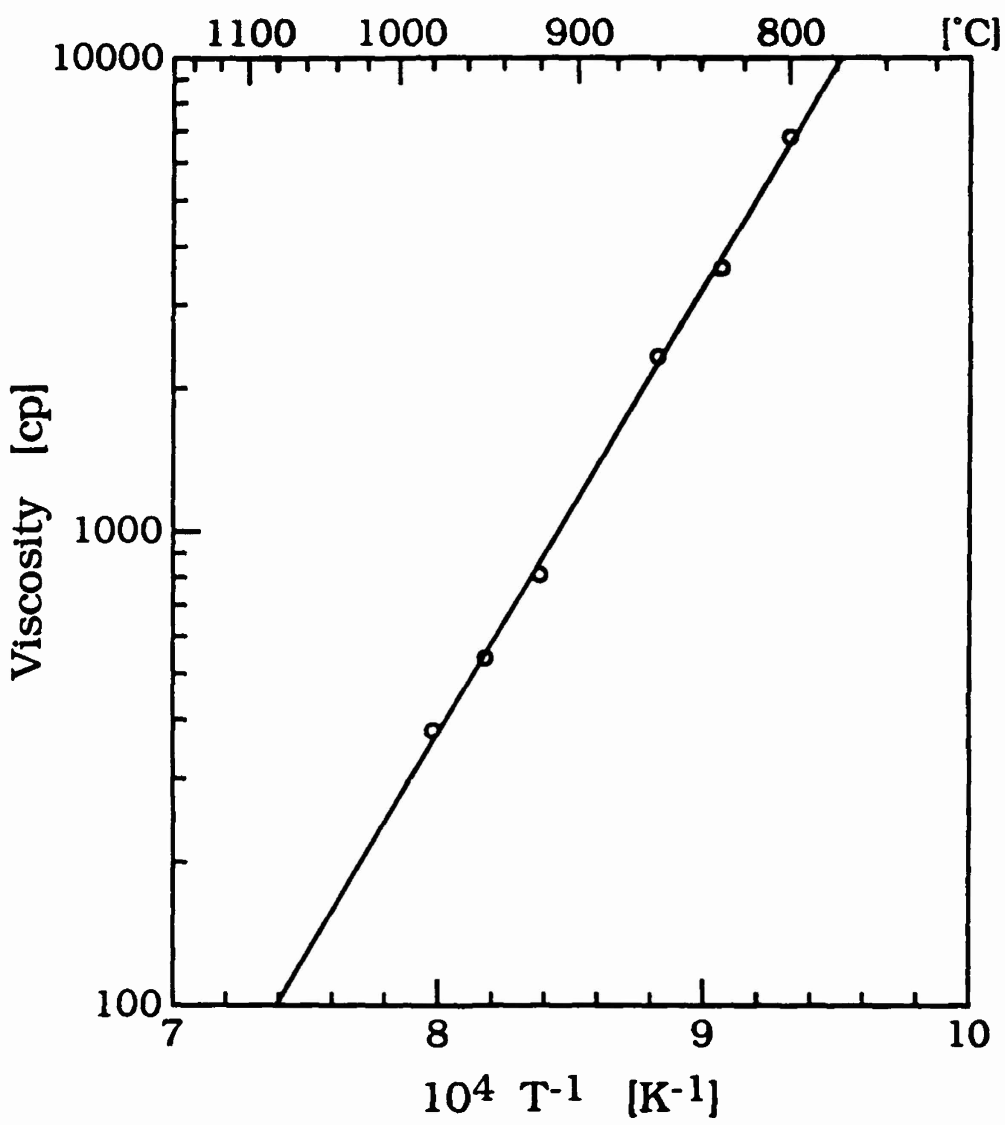


Fig. 3. Viscosity of a 10 wt%  $\text{Li}_2\text{O}$  - 90 wt%  $\text{B}_2\text{O}_3$  growth solution with liquidus near 800°C.

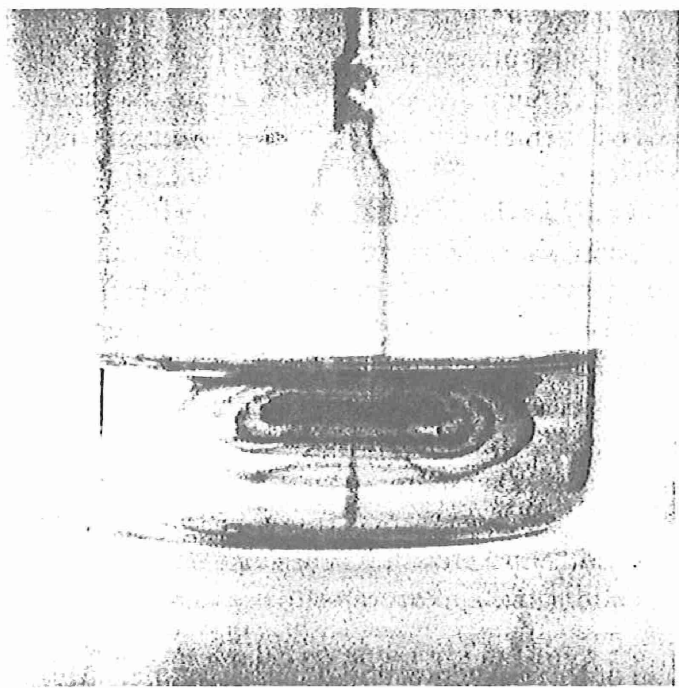


Fig. 4. Flow pattern in water-glycerol solution of 1 poise viscosity. LBO growth solutions range as high as 100 x this value and consequently would exhibit even less mixing due to seed rotation.

the likelihood of secondary nucleation due to spurious crystallites on the seed surface, and it reduced the occurrence of spontaneously-nucleated crystallites on the melt surface.

Almost all the growth experiments were carried out with some degree of seed pulling in order to achieve boules of greater length than is the usual case when seed pulling is not used. The TSSG method has a general tendency to produce shallow lens-shaped boules less than 20 mm thick, and this limits maximum crystal dimensions to even shorter lengths because of the need to cut them along specific phase matching directions.

Crystals were evaluated after growth by optical methods since we were interested primarily in macroscopic crystal quality in the bulk of these experiments. X-ray powder diffraction analysis was relied on for phase identification and verification.

### 5. Results

Once the problem of seeding and initiation of growth was solved, the growth of single crystal boules of LiB<sub>3</sub>O<sub>5</sub> from Li<sub>2</sub>O-B<sub>2</sub>O<sub>3</sub> solutions using the TSSG method was found to be relatively straightforward. Growth rates had to be maintained at minimal levels in order to avoid the occurrence of cellular breakdown on the growth interfaces, however, and this limited cooling rates to the order of 1° C/day. Typically, crystals could be pulled on the order of 0.5 mm/day during the entire 2-3 week growth interval.

It was found that growth anisotropy in LBO is stronger than it is in BBO, and crystals grown without pulling tended to remain strongly faceted as they grew to significant fractions of the crucible diameter. A photograph of a c-axis crystal grown without pulling is shown in Fig. 5, where its mm orthorhombic symmetry is clearly visible. This crystal developed additional grains during growth. Unpulled crystals were often observed to incorporate secondary grains that nucleated spontaneously and floated on the melt surface. While they tended to line up with, and incorporate on existing facets, they usually produced highly strained boundaries that caused fractures upon cooling. Crystals grown with pulling from the very beginning of growth tended to round out when their diameters became large enough that the volume pulled per unit time equaled the volumetric amount of solute (LBO) rejected from the growth solution per unit time due to the slow cooling imposed on the system. Seed orientation was found to influence the faceting as well. Growth normal to the (101) plane resulted in oval cross-section crystals that could be pulled rather successfully, Fig. 6. Growth normal to the (010) plane, in contrast, resulted in a highly faceted habit that was not suitable for pulling. Pulled crystals all exhibited some degree of undercutting if constant cooling and pulling rates were used. By calculating the yield of solid material per degree of cooling, it was possible to adjust the growth parameters during

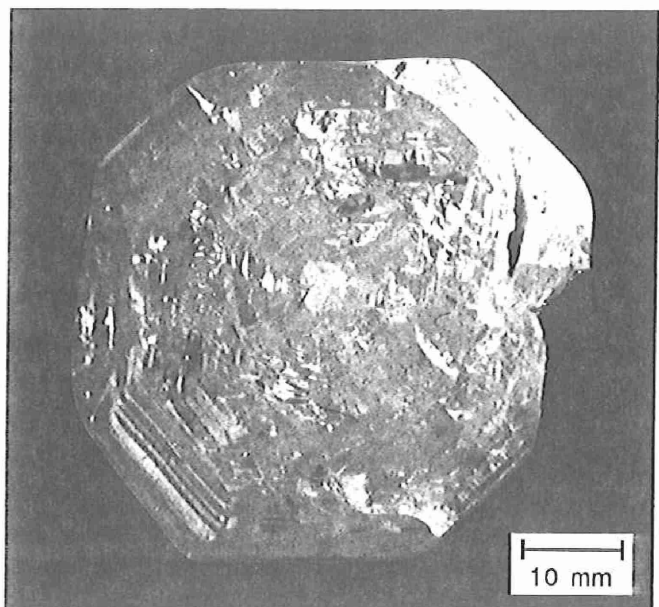


Fig. 5. C-axis crystal grown with minimal pulling.

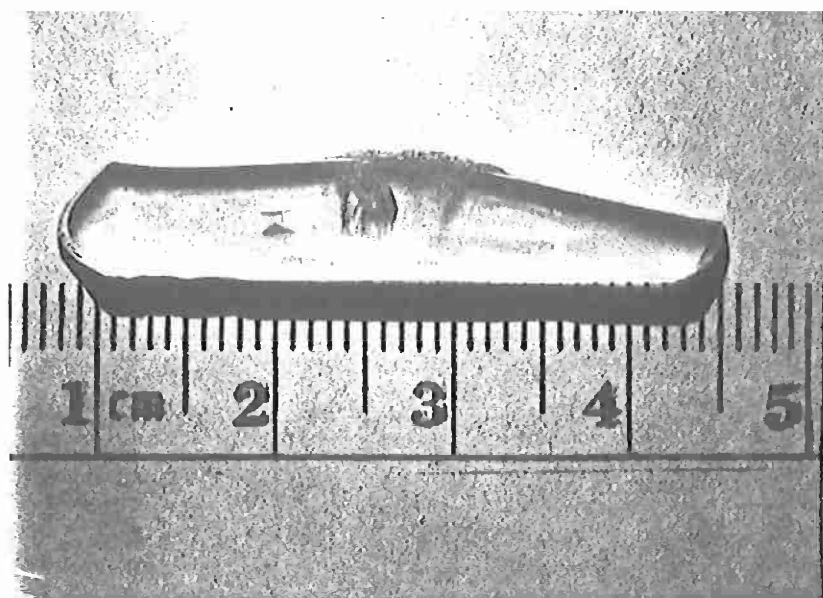


Fig. 6. Cross-section of LBO crystal grown in the (101) crystallographic direction.

the growth run to minimize this effect. The most successful seed orientation was the c-axis (001) since it was possible to pull crystals in lengths greater than 15 mm by adjusting growth parameters accordingly, Fig. 7.

Although a few localized defects that may be either voids or inclusions were found in these crystals, the yield of useable optical specimens appeared to be much higher than from typical BaB<sub>2</sub>O<sub>4</sub> crystals.

Occasional mention is found in the literature of surface decomposition and LBO crystals cracking during the cooling cycle after growth.<sup>[13,14]</sup> The cracking phenomenon has generally been attributed to the large thermal expansion anisotropy recently been documented in LBO.<sup>[13]</sup> Post-growth cracking was observed in many of our crystals, as well, but it was always found to be more extensive on the tops of the crystals, which are exposed to the ambient atmosphere as the crystals are pulled from the melt. Generally, after several days, the top surfaces of a number of our crystals developed a thin, patchy film with a cloudy appearance. This thin film tended to grow in thickness and lateral extent during the entire growth process, eventually covering the free surface of the crystal with a millimeter thick, optically opaque polycrystalline layer. Cross-sectional microscopic examination of LBO seeds that were loosely surrounded by a platinum holder during the growth process indicated that this layer also formed on the seeds and appeared to be a reaction product rather than a deposit. It appeared to cause little problem during growth other than to prevent visual monitoring of the crystal's optical quality, while slowly eroding the seed cross-section. However, after growth, closely associated variable cracking always occurred irrespective of how slowly the furnace was cooled to room temperature, Fig. 8. The polycrystalline surface layers were obviously quite fragile and would not likely have had the tensile or compressive strength necessary to fracture an intact single crystal multi-centimeters in dimension, and few other indications as to the role of this layer in the fracturing phenomenon were found during the course of this program. {After this program's conclusion, research on the growth of LBO was intensified with support from DARPA and ultimately a solution to the surface decomposition problem was found.<sup>[15]</sup> This advance, which followed from the groundwork provided here has increased the yield of LBO crystals and is considered a major improvement in the growth technology of LBO.}

## 6. Discussion

The most significant challenge encountered in the growth of LBO crystals from B<sub>2</sub>O<sub>3</sub> solutions was the problem of avoiding interface breakdown, which necessitated the use of the very low growth rates mentioned (less than 1° C/day). Crystals that were

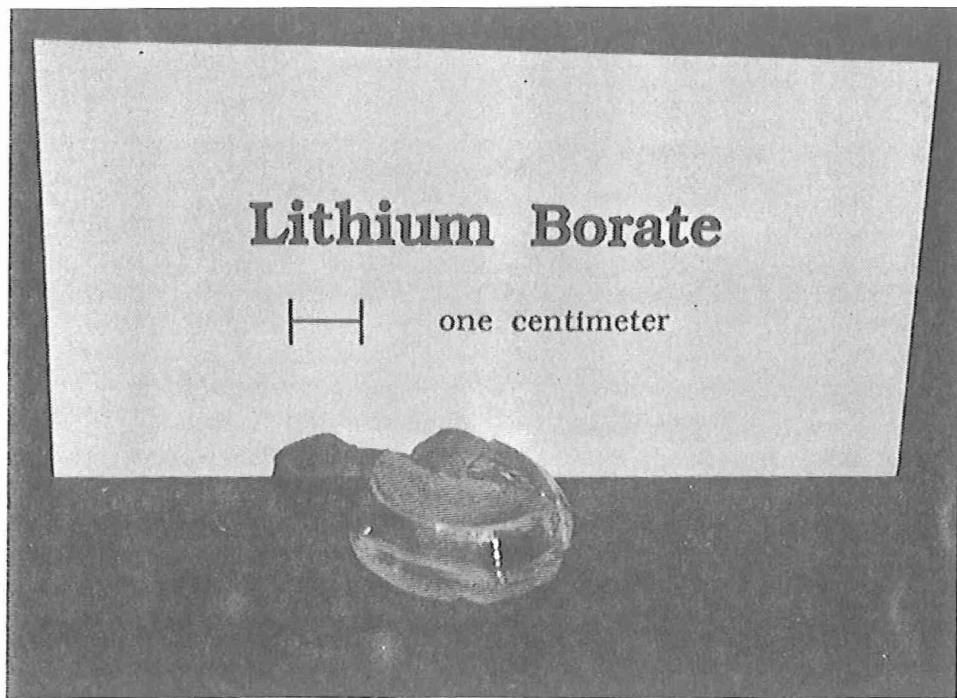


Fig. 7. Early  $\text{LiB}_3\text{O}_5$  single crystal grown from a  $\text{B}_2\text{O}_3$  solution along the [001] crystallographic direction. Fracturing was caused by a small amount of flux adhering to the bottom of the crystal as it was pulled from the melt.

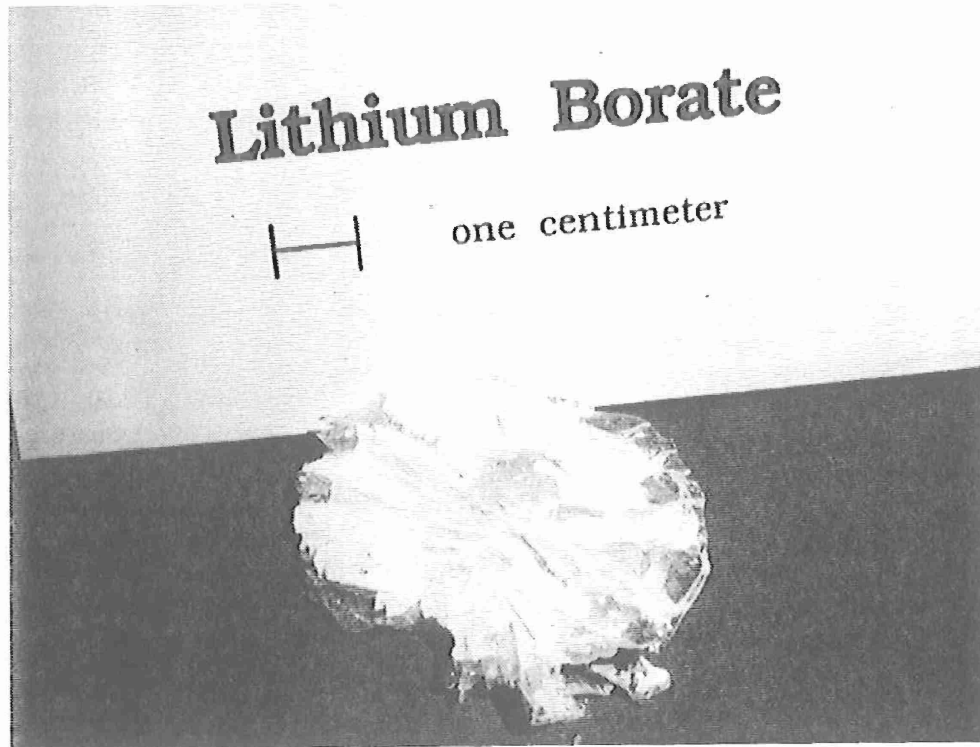


Fig. 8. Cross-sectional study of LBO seed after growth showing that a very significant fraction of its original cross-section had decomposed during the growth process. (Once seed decomposition is complete, mechanical attachment to the crystal is lost and it is rarely possible to retrieve the crystals from the growth solutions when that happens.)

cooled significantly faster than this, or that were inadvertently pulled faster than their corresponding linear growth rates allowed, inevitably developed unstable, cellular growth interfaces due to constitutional supercooling. This was assumed to be due mainly to mass transport limitations caused by the extremely high melt viscosities. Forced convective stirring through seed rotation was found to be relatively ineffective, and the preliminary experiments on viscosity modification did not indicate clear advantages over the pure B<sub>2</sub>O<sub>3</sub> unmodified solvent.

In slowly grown c-axis crystals, a core several millimeters in diameter consisting of solvent inclusions and/or voids often occurred. This feature, also seen in TSSG-grown BBO crystals, is due to localized fluid stagnation at the center of the growth interface. Farther out from the crystal axis, relatively few macroscopic optical defects were found. Significantly less optical scatter was observed in the "interface stable" LBO crystals than was typically seen in "interface stable" BBO crystals. This difference was surprising since the viscosities of the LBO melts used were very much higher than typical Na<sub>2</sub>O-based BBO melts, and one might, therefore, anticipate a greater density of solvent inclusions in the case of LBO. We had earlier postulated that, in the case of BBO, because of the occurrence of widely distributed solvent inclusions far from regions of interface instability which are clearly caused by constitutional supercooling, a second solvent inclusion mechanism may exist, [16] and that this could account for the enhanced optical scatter seen in BBO crystals.

The yield from these early crystals was quite good. High power, high efficiency resonant second harmonic generation of the 1.06 μm line was demonstrated at Stanford using an 11 mm long optical LBO crystal grown here, [3] and a series of crystals has also been fabricated in order to determine the temperature dependent Sellmier coefficients for this material.

#### 7. Summary of Results

1. Multi-centimeter diameter LiB<sub>3</sub>O<sub>5</sub> crystals up to 15 mm in length have been grown from 10 wt % Li<sub>2</sub>O - 90 wt % B<sub>2</sub>O<sub>3</sub> solutions using both c-axis (001) and (101) seeds.
2. High thermal gradient TSSG furnaces like those used for the growth of BBO were used successfully for the growth of good quality LBO crystals, but only at cooling rates less than 1° C/day and linear growth rates of less than 1 mm/day. Pulling, as long as it was initiated at the beginning of the growth cycle, was found to result in longer boules with higher yields than unpulled boules.

3. With the exception of a 1-2 mm core region that did have a high density of (solvent) inclusions, relatively few optical defects due to solvent inclusions were found elsewhere in the crystals.
4. Melts with excess B<sub>2</sub>O<sub>3</sub> as the solvent were found to have very high viscosities, and mass transport was, therefore, concluded to be the rate limiting mechanism in this system. Limited experiments using flux modifiers did not result in improved crystal quality or an increase in maximum allowable growth rate. Reduced melt viscosities through the identification of a more suitable flux modifier should be pursued, however, as a means to increase the maximum allowable growth rates.

#### 8. References: Part B

1. C. Chen, Y. Wu, A. Jiang, B. Wu, G. You, R. Li, and S. Lin, "New nonlinear-optical crystal: LiB<sub>3</sub>O<sub>5</sub>," J. Opt. Soc. Am. **6** (4), 616-621 (April 1989).
2. J. P. Chernoch, M. J. Kokla, W. T. Lotshaw, and J. R. Unternahrer, "High average power second harmonic generation in lithium triborate (LBO), Soc. for Optics & Quantum Elec., Proc. from Lasers '91, STS Press, McLean, VA (1991).
3. S. T. Yang, C. C. Pohalski, E. K. Gustafson, R. L. Byer, R. S. Feigelson, R. J. Raymakers, and R. K. Route, "6.5 watt cw 532 nm radiation by resonant external cavity SHG of an 18 watt Nd:YAG laser in LBO," Proc. of IEEE/OSA Conf. on Advanced Solid State Lasers, Hilton Head, S. Carolina, March 18-22, 1991.
4. C. Mazzetti and F. D. Carli, Gazz. Chim. Ital. **56**, 23 (1926).
5. A. P. Rollet and R. Bouaziz, Compt. Rend. (Paris) **240**, 2417 (1955).
6. H. König and R. Hoppe, Z. Anorg. Allg. Chem. **439**, 71 (1978).
7. B. S. R. Sastry and F. A. Hummel, J. Am. Ceram. Soc. **41**, 11 (1958).
8. A. Jiang, T.-b. Chen, Y. Zheng, Z.-s. Chen, S.-a. Wang, F. Chen, J.-j. Lin, D.-M. Ke, and Y.-f. Lin, "Growth of a new nonlinear optical crystal-lithium triborate, abstract."
9. C. Chen, et al., "LiB<sub>3</sub>O<sub>5</sub> crystal and its nonlinear optical devices," U.S. Patent No. 4,826,283 (1989).
10. Private communication with B. H. T. Chai (1990).
11. L. Shartsis, W. Capps and S. Spinner, "Viscosity and electrical resistivity of molten alkali borates," J. Amer. Cer. Soc. **36** (10), 319 (Oct. 1, 1953).
12. S. Zhao, C. Huang and H. Zhang, "Crystal growth and properties of lithium triborate," J. Crystal Growth **99**, 805-810 (1990).

13. W. Lin, G. Dai, Q. Huang, A. Zhen, and J. Liang, "Anisotropic thermal expansion of  $\text{LiB}_3\text{O}_5$ ," (April 6, 1990).
14. D. Tang, Q. Lin, W. Zheng, C. He, J. Wang, X. Lin, and H. Hong, "Study on growth of lithium triborate (LBO) single crystals," Proc. of 9th Chinese Conf. on Crystal Growth & Mat., Huangshan, China, Sept. 1991.
15. E. Brück, R. J. Raymakers, R. K. Route, and R. S. Feigelson, "Surface stability of lithium triborate crystals grown from excess boric oxide solutions," in submission to *J. Crystal Growth*.
16. R. S. Feigelson, R. J. Raymakers and R. K. Route, "Solution growth of barium metaborate crystals by top-seeding," *J. Crystal Growth* **97**, 352-355 (1989).

### C. SILVER GALLIUM SELENIDE

#### 1. Objectives

Program objectives relating to silver gallium selenide were to improve its optical quality by developing a better heat-treatment procedure for removing the optical scattering centers from as-grown crystals. We sought to do this through an increased understanding of the chemistry, the mass transport and kinetics of the heat-treatment process.

#### 2. Background

Single crystals of  $\text{AgGaSe}_2$  with high optical quality have potentially important infrared nonlinear optical applications.<sup>[1]</sup> However, due to an off-stoichiometric congruency,  $\text{AgGaSe}_2$  always grows slightly rich in  $\text{Ga}_2\text{Se}_3$  in accordance with the known phase equilibria in the  $\text{Ag}_2\text{Se}$ - $\text{Ga}_2\text{Se}_3$  pseudobinary system.<sup>[2,3]</sup> This inevitably leads, upon cooling, to the formation of  $\text{Ga}_2\text{Se}_3$ -rich precipitates that cause appreciable optical scattering in the near-infrared wavelength ( $0.73$ - $2 \mu\text{m}$ ) region. The precipitates can be eliminated either by quenching or heat-treating the crystals in the presence of  $\text{Ag}_2\text{Se}$ .<sup>[3]</sup> In the quenching technique, as-grown crystals are cooled rapidly to room temperature from an elevated temperature. Although effective in eliminating the precipitates, quenching usually leads to cracking of the crystals. For this reason annealing in the presence of  $\text{Ag}_2\text{Se}$ , which causes less damage to the crystals, is preferred.

Several variations to the annealing techniques have been reported, depending on whether or not there is contact between the crystal and annealing medium, or whether there was an annealing medium present at all.<sup>[3-6]</sup> Nonetheless, a systematic analysis of the heat treatment process had not yet been developed. In our laboratory, analyses of the chemical reaction products and the condensed volatile species found within the heat treatment ampoule in the temperature range of  $500^\circ\text{C}$  to  $800^\circ\text{C}$  had revealed no significant differences between the contact and the contactless cases. However, for complete elimination of the precipitate phase, it was empirically determined that direct contact was necessary. To gain a better understanding of this behavior, we set out to analyze the chemical reactions that occur during the heat-treatment process, and to determine the chemical interdiffusion coefficients for the mobile species. We also undertook to develop a chemical mass balance model that would make it possible to predict the kinetics of the heat treatment process from fundamental parameters.

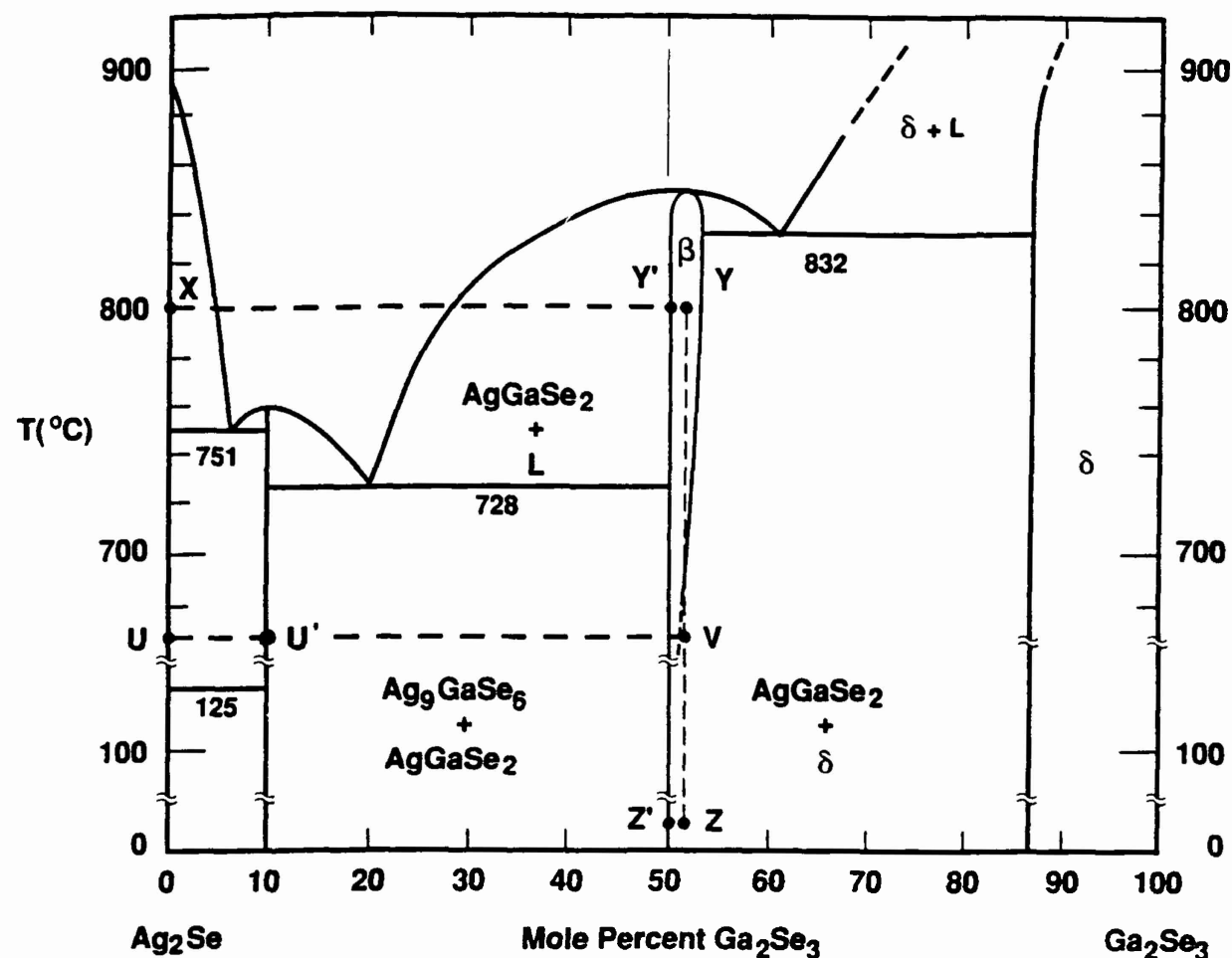


Fig. 1. Phase equilibria in the  $\text{Ag}_2\text{Se}-\text{Ga}_2\text{Se}_3$  pseudobinary system after Mikkelsen [2] showing the 800  $^{\circ}\text{C}$  diffusion couple (X-Y) used during commercial heat-treatment processing and the two isoconcentration cooling paths followed by as-grown cloudy crystals (Y-Z) and heat-treated clear crystals (Y'-Z'). The line (U-V) represents the low temperature diffusion process evaluated in this study.

### 3. Chemical Analysis of the Heat-Treatment Process

To develop a quantitative model for the heat-treatment procedure that is necessary for eliminating the precipitate phase from  $\text{AgGaSe}_2$  crystals, we first undertook to analyze the process using microchemical analytical techniques, low temperature processing, and reactive diffusion couples which could be analyzed after heat-treatment by x-ray diffraction, optical microscopy and electron probe microanalysis.

The most common high temperature heat-treatment process for eliminating second phase precipitates utilizes a binary diffusion couple which places  $\text{AgGaSe}_2$  crystals in direct contact with a small amount (approximately 1.0 mol%) of  $\text{Ag}_2\text{Se}$  for three weeks at 800°C in an evacuated and sealed quartz ampoule,<sup>[6]</sup> as indicated by the line X-Y on the phase diagram shown in Fig. 1. Since the  $\text{AgGaSe}_2$  is usually placed on top of the  $\text{Ag}_2\text{Se}$  to ensure good physical contact, the annihilation of second-phase precipitates is expected to proceed from the bottom of the crystal to the top, and thus the transparency of the  $\text{AgGaSe}_2$  crystal to be greater at the bottom than at the top until the diffusion process has gone to completion. However, dark field IR scattering measurements using a silicon vidicon imaging technique<sup>[6]</sup> showed that annihilation proceeds uniformly inward from all free surfaces of the crystal, regardless of the distance to the  $\text{Ag}_2\text{Se}$  annealing medium. Previous studies in our laboratory had demonstrated that vapor phase transport plays only a minor role in the heat treatment process, and this behavior was therefore puzzling.

In this study, chemical reactions occurring during heat-treatment were analyzed at several temperatures below the eutectic temperature using reactive diffusion couples<sup>[7-9]</sup> between as-grown  $\text{AgGaSe}_2$  crystals and polycrystalline  $\text{Ag}_2\text{Se}$  (indicated by the line U-V in Fig. 1), and standard (chemical inter-) diffusion couples between as-grown  $\text{AgGaSe}_2$  crystals and polycrystalline  $\text{Ag}_9\text{GaSe}_6$  (indicated by line U'-V'), an intermetallic compound in the  $\text{Ag}_2\text{Se}-\text{Ga}_2\text{Se}_3$  pseudobinary system that is in phase equilibrium with stoichiometric  $\text{AgGaSe}_2$ .<sup>[2]</sup> In the reactive diffusion couples that are representative of the commercial heat-treatment process, but which were processed in this study at a lower temperature to avoid complications caused by the formation of a liquid phase at the interface, we observed formation of the intermediate  $\text{Ag}_9\text{GaSe}_6$  phase both normal to the mechanical interface, and along the free surface. Analyzing the microchemical analytical data to determine the relative surface and volume diffusivities for silver,  $D_s^{\text{Ag}}$  and  $D_v^{\text{Ag}}$  respectively, we found:

$$D_s^{\text{Ag}} = 5.43 \times 10^{-4} \exp(-0.46 \text{ eV/kT})$$

$$D_v^{\text{Ag}} = 2.40 \times 10^{-7} \exp(-0.84 \text{ eV/kT})$$

It can readily be seen that at all temperatures, surface diffusivities were much larger than volume diffusivities.

Initially, it was assumed that Ag would turn out to be the principal mobile species. It was found, however, that the volume diffusivities for Ga and Se in the  $\text{AgGaSe}_2$  phase were approximately the same as that for Ag. We also found that the volume diffusivity of Ag at 700° C (approximately  $1 \times 10^{-11} \text{ cm}^2/\text{s}$ ) was much lower than typical values for Ag diffusivity at 700° C in GaAs (approximately  $3 \times 10^{-8} \text{ cm}^2/\text{s}$ ) [10] and for Ag diffusivity at 700° C in  $\text{Ag}_{0.8}\text{Cd}_{0.2}\text{Te}$  (approximately  $1 \times 10^{-9} \text{ cm}^2/\text{s}$ ). [11] Self-diffusion studies of Se in CdSe [12] and chemical interdiffusion studies of Se in CdTe, [13] on the other hand, revealed diffusivities on the order of  $10^{-11} \text{ cm}^2/\text{s}$  at 700° C, much closer to the values determined in this study. Since our experimental diffusivities are more characteristic of Se (anion) rather than Ag (cation) diffusion, we postulate that the diffusivities measured here are those resulting from a cooperative phenomena among Ag, Ga and Se atoms, where Se may move together with Ag and Ga to maintain binary ( $\text{Ag}_2\text{Se}$  and  $\text{Ga}_2\text{Se}_3$ ) stoichiometry and electroneutrality, and that the diffusion kinetics of Se are the rate limiting mechanism. [14]

From the experimental results of this study, the uniform annihilation of second-phase precipitates in  $\text{AgGaSe}_2$  samples during high temperature heat-treatment can be postulated to occur as follows. The intermetallic compound,  $\text{Ag}_9\text{GaSe}_6$  forms initially at the  $\text{Ag}_2\text{Se}-\text{AgGaSe}_2$  interface as a result of reactive diffusion, rapidly covers the entire surface of the  $\text{AgGaSe}_2$  sample before significant volume diffusion occurs because of the high rate of surface diffusion. This effect is shown in Fig. 2. (The formation of a liquid phase during high temperature heat-treatment processing may even facilitate the surface migration process beyond that observed here.) Volume diffusion of the Se anion with its slower kinetics then becomes the rate limiting mechanism in the heat treatment process, and this accounts for the fact that diffusion appears to proceed uniformly inward from all surfaces of the crystal.

It is still not known what defect allows for the excess solubility of  $\text{Ga}_2\text{Se}_3$  in  $\text{AgGaSe}_2$  at elevated temperatures, nor is it known for certain whether this  $\text{Ga}_2\text{Se}_3$  excess is eliminated through out-diffusion of  $\text{Ga}_2\text{Se}_3$  or by in-diffusion of  $\text{Ag}_2\text{Se}$ . Mass balance studies on the closely-related nonlinear material,  $\text{AgGaS}_2$  have demonstrated that  $\text{Ga}_2\text{S}_3$  does in fact out-diffuse from the matrix during heat-treatment processing. Preliminary studies in our laboratory have indicated that the selenide system may behave similarly, but

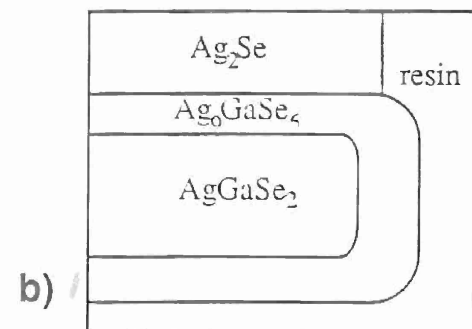
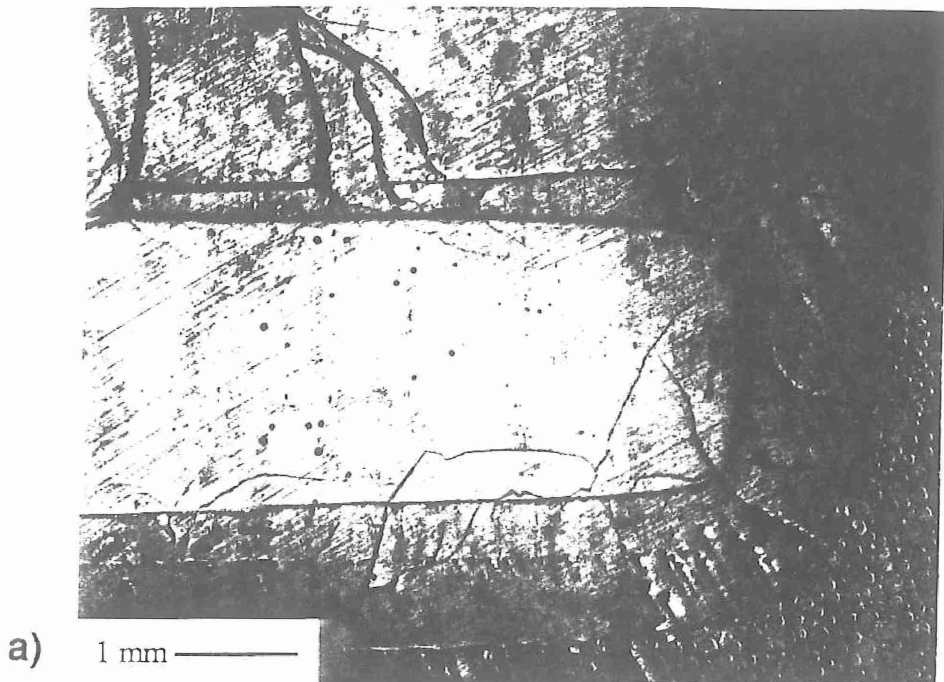


Fig. 2. a) Optical micrograph, and b) illustration showing the formation and rapid surface migration of the  $\text{Ag}_9\text{GaSe}_6$  phase at the junction of an  $\text{Ag}_2\text{Se}$ - $\text{AgGaSe}_2$  reactive diffusion couple. Here, the  $\text{Ag}_9\text{GaSe}_6$  phase has completely enveloped the  $\text{AgGaSe}_2$  phase. The cracks, which originated in the polycrystalline  $\text{Ag}_2\text{Se}$  phase, have propagated through the  $\text{Ag}_9\text{GaSe}_6$  phase during cooling.

this has not yet been unambiguously demonstrated and further investigation in this area is warranted.

*This particular research topic is described in greater detail in publication number 6.*

#### 4. A Chemical Mass Balance Model for the Heat-Treatment Process

Several kinds of heat treatment experiments were carried out in resistance furnaces using centimeter size, as-grown silver gallium selenide crystals vacuum sealed in clean fused quartz ampoules with either  $\text{Ag}_2\text{Se}$  or  $\text{Ag}_9\text{GaSe}_6$  present as an annealing medium. Crystals and the annealing medium were weighed to  $\pm 10^{-4}$  g before and after heat-treatment processing in order to determine the magnitude and direction of mass transport. To quantify the contribution of vapor transport to the heat-treatment process, we studied a contactless process in which only vapor phase transport could occur, as well as the usual contact case in which both vapor phase transport and diffusive transport could occur. In the noncontact case, heat-treatment was performed at  $800^\circ \text{C}$ , well above the eutectic ( $728^\circ \text{C}$ ) [2] in order to maximize the amount of transport.

In the cases where the crystals and the annealing medium were in direct mechanical contact, heat-treatment had to be carried out below the eutectic temperature ( $728^\circ \text{C}$ ) in order to prevent the formation of a liquid phase, which would have complicated the problem of separating the crystals from the annealing medium afterward. (It was essential that they be separated cleanly afterward in order to accurately determine the final weight of each.) Crystals in these experiments were placed on top of the annealing media in order to insure a constant pressure holding them together. Direct contact annealing was typically carried out at  $670^\circ \text{C}$  for 7 days.

After heat treatment, the ampoules were opened, the crystals carefully separated from any annealing media present, and weighed using a microbalance. A Norelco powder x-ray diffractometer analyzed for phase content. Many of the crystals developed a thin surface film during processing, and this was analyzed with a four circle x-ray diffractometer in order to determine its chemical composition.

All x-ray patterns corresponded to one or more of the phases found on the pseudobinary join, indicating that in the condensed phase, pseudobinary approximation is reasonably accurate. In some cases, a slight discrepancy existed between initial and final weights, due, we concluded, to condensation of small amounts of material on the quartz ampoules. In no case did the condensed amount on the quartz wall exceed 3% of the total mass transported during processing.

We analyzed the experimental results with a chemical mass balance relying upon the following assumptions:

- (a) The  $\text{Ga}_2\text{Se}_3$ -rich precipitates occurring during the crystal growth of  $\text{AgGaSe}_2$  have the composition  $\text{AgGa}_7\text{Se}_{11}$  in accordance with the known phase equilibria in the system. [2,3]
- (b) The concentration of the precipitate phase in as-grown crystals is approximately 0.5 mol %. [15]
- (c) There is no solid solubility between  $\text{Ag}_2\text{Se}$  and  $\text{Ag}_9\text{GaSe}_6$ , or between  $\text{Ag}_9\text{GaSe}_6$  and  $\text{AgGaSe}_2$ , consistent with the  $\text{Ag}_2\text{Se}$ - $\text{Ga}_2\text{Se}_3$  phase diagram.
- (d) When as-grown  $\text{AgGaSe}_2$  crystals containing precipitates are heated up above the solvus, a solid solution of  $\text{AgGaSe}_2$  and  $\text{AgGa}_7\text{Se}_{11}$  is formed, which means that the precipitates redissolve in the crystal.
- (e) When vapor transport occurs during heat-treatment from the crystal toward the annealing medium, it is not clear which species is moving. Several possibilities include  $\text{Ga}_2\text{Se}_3$ ,  $\text{Ga}_2\text{Se}$ ,  $\text{GaSe}$  and  $\text{Ga} + \text{Se}$  atoms. [16] From the previous research and our annealing experiments, it was clear that the  $\text{AgGa}_7\text{Se}_{11}$  precipitates in as-grown crystals were eliminated and that the crystals lost weight. This means that the weight loss of the crystal is directly related to the combination of two Ga atoms with three Se atoms. Thus, even though the exact transporting species is/are not known, we assume that the weight change of the crystal before and after annealing is due to the mass transport in the 2Ga:3Se ratio.
- (f) When there is diffusive transport (contact annealing), the number of moles of 2Ga:3Se vapor transported to the annealing medium is negligible compared to that of  $\text{Ag}_2\text{Se}_3$  transported to the crystal. This was clearly demonstrated in the diffusivity determinations described in section 3 above.

By applying these assumptions and a simple mass transport model to the low temperature heat-treatment experiments, we were able to deduce the following:

- (a) The diffusive transport process can be decoupled from the vapor transport and the relative contribution of each can be accurately determined.
- (b) The rate of elimination of precipitates for contact heat-treatment is much faster than that for contactless heat-treatment because the former involves an additional diffusive transport component. Furthermore, the diffusive term becomes predominant as the heat-treatment temperature increases because vapor transport has a Knudsen type

$\exp(-a/T)/T^{1/2}$  dependence, [17] while diffusive transport has an Arrhenius type  $\exp(-b/T)$  dependence, [10,18,19] where a and b are constants.

(c) The heat-treatment processes can be controlled by varying the annealing temperature, annealing time, and the amount of annealing medium.

(d) The formation of an intermediate  $\text{Ag}_9\text{GaSe}_6$  phase which inevitably damages the surfaces of silver gallium selenide crystals during high temperature contact annealing can be eliminated by using  $\text{Ag}_9\text{GaSe}_6$  itself as the annealing medium at temperatures below the eutectics in the system.

At higher temperatures in the 800° C range, which is typical of the commercial heat-treatment process, it was not possible to separate the two components of mass transport in the contact case because of liquid phase formation. It was possible, however, to analyze the transport phenomena in the contactless case where vapor transport is the only process occurring.

Four steps were assumed to be involved in the contactless annealing case: (i) the dissolution of  $\text{AgGa}_7\text{Se}_{11}$  precipitates into a solid solution, (ii) out-diffusion of  $\text{Ga}_2\text{Se}_3$ , (iii) transport of 2Ga:3Se through the vapor phase, and (iv) a chemical reaction between 2Ga:3Se and the annealing medium.

The overall reaction rate at high temperature depends on the slowest steps of these. It was found that vapor transport was the rate determining step, and thus the flux (and the rate of mass transport) could be described by the Knudson equation, [17]

$$J = \frac{0.0226 \exp(-\frac{34313}{RT})}{\sqrt{T}} .$$

The following data supported this conclusion. Contactless annealing of a 2.2301 g crystal at 600° C for 7 days resulted in a weight change of 0.0015 g. By carefully measuring its surface area, the flux of 2Ga:3Se was calculated to be  $2.05 \times 10^{-12} \text{ mol/cm}^2 \text{ sec}$ . The predicted flux using the Knudson equation was  $1.96 \times 10^{-12} \text{ mol/cm}^2 \text{ sec}$ , very close to the experimental value.

The vapor transport process is slower than out-diffusion of excess  $\text{Ga}_2\text{Se}_3$  from the crystal, and therefore it determines the kinetics of the contactless heat treatment process.

*This particular research topic is described in greater detail in manuscript number 1.*

### 5. Summary of Results

The kinetics involved in the heat treatment process have been analyzed using a chemical mass balance model. Heat treatment at two temperatures was studied; several low temperature cases involving both contactless and contact processing, and one high temperature case involving contactless processing. Quantitative mass transport measurements for contact annealing and for contactless annealing permitted us to decouple the diffusive transport contribution from vapor transport, contribution and determine the kinetic differences between the contact and contactless cases. Diffusive transport was found to be significantly faster than vapor phase transport, and this explains why contact annealing appears to be more effective than contactless annealing for elimination of precipitates. The chemical mass balance model and the phase identification XRD studies suggests that the mobile species is  $\text{Ga}_2\text{Se}_3$ , and that it plays the dominant role in the elimination of the precipitates from as-grown  $\text{AgGaSe}_2$  crystals. The basic mechanism and fundamental constants that control the vapor transport process during contactless heat treatment at high temperature were determined. These, together with a diffusion model that makes use of the diffusivity measurements reported in the previous section, comprise a reasonably complete quantitative understanding of the heat treatment process.

### 6. References: Part C

1. J. L. Shay and J. H. Wernick, *Ternary Chalcopyrite Semiconductors: Growth, Electronic Properties, and Applications*, Pergamon Press, New York (1975), Ch. 1.
2. J. C. Mikkelsen, Jr., Mat. Res. Bull. **12**, 497-502 (1977).
2. J. L. Shay and J. H. Wernick, Ternary Chalcopyrite Semiconductors - Growth, Electronic Properties and Applications, Ch. 1, (Pergamon Press, 1975).
3. R. K. Route, R. S. Feigelson, R. J. Raymakers, and M. M. Choy, J. Crystal Growth **33**, 239-245 (1976).
4. N. B. Singh, R. H. Hopkins, and J. D. Feichtner, J. Mat. Sci. **21**, 837-842 (1986).
5. N. B. Singh, R. H. Hopkins, R. Mazelsky, and H. H. Dorman, Mat. Letters **4** (8-9), 357-359 (1986).
6. R. S. Feigelson and R. K. Route, Mat. Res. Bull. **25**, 1503-1511 (1990).
7. B. Y. Pines, Soviet Phys.-Solid State **1**, 434-437 (1959).
8. B. Y. Pines, and E. F. Chaikovskii, Soviet Phys.-Solid State **1**, 864-869 (1959).

9. S. Mrowec, *Defects and Diffusion in Solids*, Elsevier, 1980, Ch. 2.
10. D. L. Kendall, *Semiconductors and Semimetals*, Academic Press, New York (1968) **4**, Ch. 3.
11. M. S. Tang, Ph. D. Thesis, Stanford University (1987).
12. H. Kato, M. Yokozawa, and S. Takayanagi, Japan. J. Appl. Phys. **4**, 1019 (1965).
13. H. H. Woodbury and R. B. Hall, Phys. Rev. **157**, 641 (1967).
14. M. S. Tang and D. A. Stevenson, J. Phys. Chem. Solids **51**(6), 563-569 (1990).
15. Private communication with J. Heitanen, Cleveland Crystals, Inc. (1990).
16. David R. Lide (Ed.), CRC Handbook of Chemistry and Physics, 72nd ed., CRC Press, 1991.
17. M. Knudsen, Ann. Phys. **47**, 697 (1915).
18. G. Neumann and G. M. Neumann, *Diffusion Monograph Series*, Ohio (1972), No. 1.
19. D. Shaw, J. Crystal Growth **86**, 778-796 (1988).

### **III. CONCLUSIONS AND RECOMMENDATIONS FOR FURTHER STUDY**

Toward our original goals relating to the growth of BBO and LBO, this program has been very successful. Beginning with little more than the published phase equilibria in these two systems, we were able to develop effective high temperature solution growth techniques that produced large, high optical quality boules suitable for property determinations and device research. These, literally, were the first BBO and LBO crystals grown in the U. S., and we were able to provide these to Stanford's device researchers under Professor R. L. Byer within a year of initiating crystal growth studies on each. His research group was, in turn, able to demonstrate important device applications and make more accurate property determinations than were possible at the time because of limited access to crystals grown in the P.R.C.

Our program was the first to demonstrate that the optical scattering defects found in all BBO crystals at the time were due to solvent inclusions. A high thermal gradient growth technique allowed us to achieve maximum growth rates while minimizing the solvent inclusion density. Novel stirring experiments using periodic reversals in seed rotation revealed the importance of maintaining effective melt sweeping across the growing crystal interface, and it pointed out an important avenue for further study toward reducing the residual scattering losses in this material.

The growth technology for LBO is still not as advanced as it is for BBO simply because LBO is a newer material. Again using high thermal gradient furnaces, we were able to show that reasonable growth rates could be achieved while minimizing crystal defects. Like TSSG-grown BBO crystals, LBO crystals were found to have a core region containing a high density of optical defects. These were presumed to be due to solvent inclusions as well, but this was not verified due to manpower and time constraints. Our preliminary experiments on viscosity-modified growth solutions called into question literature reports that growth rates and crystal quality could be improved by using LiF as a flux additive. We found that detrimental changes in interface stability with more than a trace amount of LiF present far outweighed any possible gains that would have accrued due to the estimated reductions in melt viscosity that were achieved. Our work suggested that additional research on achieving greater melt stirring in excess B<sub>2</sub>O<sub>3</sub> melts, and on achieving better control over boule morphology of maximize cutting yields, should be pursued.

Early in this program, we transferred our BBO crystal growth technology to Cleveland Crystals, Inc. and provided them with oriented seeds with which to get started.

Throughout the program, we sought to keep them abreast of our research results and continuing developments in growth technology. In the last year of the program, we carried out a similar BBO technology transfer and an LBO technology transfer to INRAD, Inc. as well. Along the way, we sought to assist other researchers in the field when asked, and provided both information and material to Quantum Technology, Inc., in particular.

Finally, micro-chemical analytical studies on silver gallium selenide added substantially to our understanding of the heat-treatment process that is used to remove optical scattering defects (precipitates) from as-grown crystals of this material. Low temperature diffusion experiments indicated that  $\text{Ag}_9\text{GaSe}_6$  may offer advantages over  $\text{Ag}_2\text{Se}$  which is currently used in the commercial process because its use minimizes surface damage to the silver gallium selenide crystals. Further research on this low temperature alternate heat-treatment process is recommended.

#### IV. PUBLICATIONS

1. D. Y. Tang, R. K. Route and R. S. Feigelson, "The growth of barium metaborate ( $BaB_2O_4$ ) single crystal fibers by the laser-heated pedestal growth method," *J. Crystal Growth* **91**, 81 (1988).
2. R. S. Feigelson, R. J. Raymakers and R. K. Route, "Solution growth of barium metaborate crystals by top seeding," *J. Crystal Growth* **97**, 352-355 (1989).
3. R. S. Feigelson and R. K. Route, "Growth of  $\beta$ - $BaB_2O_4$  bulk crystals and fibers," *Proc. SPIE* **1104** (1989).
4. R. S. Feigelson, R. J. Raymakers and R. K. Route, "Growth of nonlinear crystals for frequency conversion," *Progress in Crystal Growth and Characterization* **20**, 115 (1990).
5. S. T. Yang, C. C. Pohalski, E. K. Gustafson, R. L. Byer, R. S. Feigelson, R. J. Raymakers, and R. K. Route, "6.5 watt cw 532 nm radiation by resonant external cavity SHG of an 18 watt Nd:YAG laser in LBO," *Optics Ltrs.* **16** (19), 1493-1495 (1991).
6. N.-H. Kim, R. S. Feigelson and R. K. Route, "Surface migration and volume diffusion in the AgGaSe<sub>2</sub>-Ag<sub>2</sub>Se system," to be published in *J. Mat. Res.* (1992).
7. Y.-X. Fan, R. C. Eckardt, R. L. Byer, J. Nolting, and R. Wallenstein, "A visible BaB<sub>2</sub>O<sub>4</sub> optical parametric oscillator pumped at 355-nm by a single-axial-mode pulsed source," *Appl. Phys. Ltrs.* **53**, 2014 (1988).
8. Y. X. Fan, R. C. Eckardt, R. L. Byer, C. Chen, and A. D. Jiang, "Barium borate optical parametric oscillator," *IEEE J-QE* **25** (6), 1196-1199 (June 1989).
9. R. C. Eckardt, H. Masuda, Y.-X. Fan, and R. L. Byer, "Absolute and relative nonlinear optical coefficients of KDP, KD\*P, BaB<sub>2</sub>O<sub>4</sub>, MgO:LiNbO<sub>3</sub>, and KTP measured by phase-matched second harmonic generation," *IEEE J-QE* **26**, 922 (1990).

\* (Research made possible with crystals grown at CMR with ARO support.)

#### Manuscripts

1. N. H. Kim, R. S. Feigelson and R. K. Route, "Heat treatment studies in silver gallium selenide (AgGaSe<sub>2</sub>) crystals," in preparation.

## V. PARTICIPATING PERSONNEL

### A. FACULTY AND STAFF

<u>Name</u>	<u>Position</u>
R. S. Feigelson	Director, Advanced Materials Processing Lab Center for Materials Research Professor (Research), Materials Science & Engineering Department
R. K. Route	Senior Research Associate
R. J. Raymakers	Research Technician
M. Wolf	Scientific & Engineering Associate
Y. Fan	Research Technician

### B. GRADUATE STUDENTS

<u>Name</u>	<u>Degrees Earned</u>
J. Brenner	M.S. (1990)
L. Moulton	Ph.D. (1991)
N.-H. Kim	Ph.D. (1992)

### C. VISITING RESEARCHERS

<u>Name</u>	<u>Institute</u>
Dr. Y. Tang	Inst. for Res. in the Structure of Matter Fujian, P.R.C.

### REPORT OF INVENTIONS AND SUBCONTRACTS

(Pursuant to "Patent Rights" Contract Clause) (See Instructions on Reverse Side)

1. NAME OF CONTRACTOR / SUBCONTRACTOR <i>CONTRACT NUMBER</i>		2. NAME OF GOVERNMENT PARTNERSHIP CONTRACTOR		3. CONTRACT NUMBER	
<b>Stanford University</b> AUG 11 1986 Jordan Quad/Birch Stanford, CA 94305-4121		<b>Dept. of the ARMY</b> Address include ZIP Code P.O. Box 12211 Research Triangle Park, NC 27709-2211			
4. AWARD DATE (YYMMDD)		5. ADDRESS (INCLUDE ZIP CODE)		6. AWARD DATE (YYMMDD)	
86-07-05		86-07-05		86-07-01	
7. TO SUBJECT INVENTIONS BEING MADE TO OR REVEALED BY CONTRACTOR / SUBCONTRACTOR (If none, so state)		8. TO SUBJECT INVENTIONS BEING MADE TO OR REVEALED BY CONTRACTOR / SUBCONTRACTOR (If none, so state)		9. TO SUBJECT INVENTIONS BEING MADE TO OR REVEALED BY CONTRACTOR / SUBCONTRACTOR (If none, so state)	
None		None		None	

10. NAME OF INVENTION(S) <i>None</i>		11. DATE OF INVENTION(S) <b>(IF NONE, SO INDICATE)</b>		12. DISCLOSURE NO. PATENT APPLICATION SERIAL NO. OR PATENT NO.	
				13. ELECTION TO FILE PATENT APPLICATIONS (1) United States (2) Foreign (3) Both (4) None	
				14. COMMERCIAL INSTRUMENT OR ASSEMBLY OR COMBINATION OF INSTRUMENTS OR ASSEMBLIES TO CIRCUMVENT UNFAIR COMPETITION	
				15. FOREIGN COUNTRIES OF OTHER APPLICATION (1) None (2) None (3) None (4) None	

16. INVENTION OR INVENTIONS NOT REVEALED BY CONTRACTOR / SUBCONTRACTOR <i>None</i>		17. NAME OF INVENTOR (Last First MI) <i>None</i>		18. DATE OF INVENTION <i>None</i>	
		19. NAME OF EMPLOYER (1) Name of Employer (2) Address of Employer (Include ZIP Code)		20. INVENTION OR INVENTIONS IN WHICH A PATENT APPLICATION WAS FILED (1) Date of Inspiration (2) Name of Employer (3) Address of Employer (Include ZIP Code)	

### SECTION II - SUBCONTRACTS (Containing a "Patent Rights" clause)

21. SUBJECT INVENTION(S) AWARDED BY CONTRACTOR / SUBCONTRACTOR (If none, so state)		22. SUBJECT INVENTION(S) AWARDED BY CONTRACTOR / SUBCONTRACTOR (If none, so state)		23. SUBJECT INVENTION(S) AWARDED BY CONTRACTOR / SUBCONTRACTOR (If none, so state)	
24. NAME OF SUBCONTRACTOR <b>(IF NONE, SO INDICATE)</b> None		25. ADDRESS (INCLUDE ZIP CODE) PR		26. SUBJECT INVENTION(S) (1) Clause Number (2) Date Received	
				27. DESCRIPTION OF WORK TO BE PERFORMED UNDER SUBJECT CONTRACT None	

### SECTION III - CERTIFICATION

28. CERTIFICATION OF AGENT OR CONTRACTOR / SUBCONTRACTOR <i>None</i>		29. SMALL BUSINESS OR NON PROFIT ORGANIZATION (If appropriate box)		30. NON PROFIT ORGANIZATION (If appropriate box)	
				31. I CERTIFY THAT THE REPORTING PARTY HAS PROCEDURES FOR PROMPT IDENTIFICATION AND TIMELY DISCLOSURE OF "SUBJECT INVENTIONS." THAT SUCH PROCEDURES HAVE BEEN FOLLOWED AND THAT ALL "SUBJECT INVENTIONS" HAVE BEEN REPORTED <b>Robert S. Feigelson</b> Principal Investigator	
				32. DATE <b>11/15/91</b>	
				33. SIGNATURE 	